JCTC Journal of Chemical Theory and Computation

Article

pubs.acs.org/JCTC

Getting down to the Fundamentals of Hydrogen Bonding: Anharmonic Vibrational Frequencies of $(HF)_2$ and $(H_2O)_2$ from Ab Initio Electronic Structure Computations

J. Coleman Howard, Jessica L. Gray, Amanda J. Hardwick, Linh T. Nguyen, and Gregory S. Tschumper*

Department of Chemistry and Biochemistry, University of Mississippi, University, Mississippi 38677-1848 United States

Supporting Information

ABSTRACT: This work presents a systematic investigation into the basis set convergence of harmonic vibrational frequencies of $(H_2O)_2$ and $(HF)_2$ computed with second-order Møller−Plesset perturbation theory (MP2) and the coupled-cluster singles and doubles method with perturbative connected triples, CCSD(T), while employing correlation-consistent basis sets as large as aug-cc-pV6Z. The harmonic vibrational frequencies presented here are expected to lie within a few cm^{-1} of the complete basis set (CBS) limit. For these important hydrogen-bonding prototype systems, a basis set of at least quadruple-ζ quality augmented with diffuse functions is required to obtain harmonic vibrational frequencies within 10 cm^{-1} of the CBS limit. In addition, second-order vibrational perturbation theory (VPT2) anharmonic corrections yield CCSD(T) vibrational frequencies in excellent agreement with experimental spectra, differing by no more than a few cm^{-1} for the intramonomer fundamental vibrations. D_0 values predicted by CCSD(T) VPT2 computations with a quadruple-ζ basis set reproduce the experimental values of $(HF)_2$ and $(H_2O)_2$ to within 2 and 21 cm^{-1}, respectively.

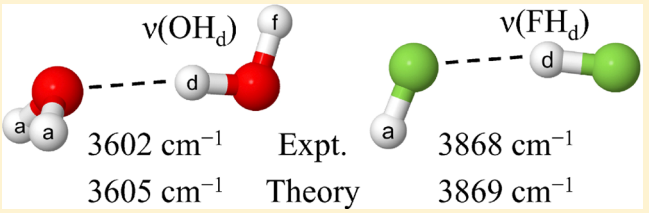

1. INTRODUCTION

Small model systems have long provided critical insight into the nature of noncovalent interactions. The interactions that stabilize these systems play crucial roles in a variety of biological and environmental phenomena.[1−3] $(H_2O)_2$ and $(HF)_2$ have served as prototypes for hydrogen bonding interactions since the first ab initio quantum mechanical (QM) calculations on H-bonded dimers in the 1960s.[4−12] The global minimum energy conformations of these dimers are depicted in Figure 1, where a mirror plane includes the nuclei

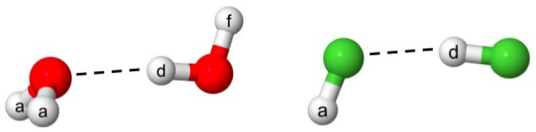

Figure 1. Global minimum geometries of $(H_2O)_2$ and $(HF)_2$.

associated with the hydrogen bond (X—H···X). The hydrogen atoms in the figure are marked to distinguish them as "donor" involved in the hydrogen bond or as a "free" or "acceptor" atom. An accurate description of the water dimer is especially important in the construction of reliable water potentials,[13−24] since the stabilizing intermonomer interactions of larger clusters are dominated by pairwise interactions.[8,25−34]

The relatively small size of these complexes makes them attractive targets for robust electronic structure methods. The computational demands of accurate coupled-cluster[35] (CC) calculations place significant limits on the number of atoms and the size of the basis set, typically requiring excitations to be limited to singles and doubles (CCSD) and possibly a perturbative treatment of the connected triple excitations as in the "gold standard" CCSD(T) method.[36] However, for $(H_2O)_2$, higher orders of electron correlation through full quadruple excitations (CCSDTQ) have been included in benchmark calculations of the dimer's interaction energy and geometry.[37,38] Relativistic and non-Born−Oppenheimer corrections have been examined with CC computations as well.[39]

Several benchmark interaction energy databases have been compiled from high-accuracy QM calculations on noncovalent dimer complexes.[40−46] By documenting the performance of lower-scaling ab initio methods or density functional theory (DFT) approximations across a diverse set of chemical systems, these databases serve as useful guides for selecting appropriate methods for larger systems. This reference data is also of interest to those designing DFT functionals or parametrizing semiempirical methods. While the collection of benchmark energetics for dimer systems in the literature is substantial, vibrational frequencies of noncovalent complexes computed from high-accuracy ab initio QM methods are far less common. Instead of comparing theory to theory, as is necessary for a quantity such as interaction energy, computed vibrational frequencies can be compared directly to an experimentally measurable property.

The additional computational effort associated with obtaining optimized molecular geometries and calculating force

Received: September 24, 2014
Published: November 19, 2014

   dx.doi.org/10.1021/ct500860v | J. Chem. Theory Comput. 2014, 10, 5426−5435

Table 1. Covalent Bond Lengths[a] and Key Intermonomer Distances (in Å) Associated with Equilibrium Monomer and Dimer Structures Optimized with CCSD(T), MP2, and CCSD Methods Using the ha5Z Basis Set

	param.	CCSD(T)	MP2	CCSD
HF monomer	R(FH)	0.9173	0.9183	0.9144
H_2O monomer	R(OH)	0.9584	0.9583	0.9555
$(HF)_2$	$R(FH_d)$	0.9230 (+0.0057)	0.9246 (+0.0063)	0.9195 (+0.0051)
	$R(FH_f)$	0.9202 (+0.0029)	0.9214 (+0.0031)	0.9172 (+0.0027)
	R(F···F)	2.7369	2.7413	2.7509
$(H_2O)_2$	$R(OH_d)$	0.9647 (+0.0063)	0.9657 (+0.0074)	0.9611 (+0.0056)
	$R(OH_f)$	0.9576 (−0.0008)	0.9574 (−0.0009)	0.9547 (−0.0009)
	$R(OH_a)$	0.9591 (+0.0007)	0.9592 (+0.0009)	0.9562 (+0.0007)
	R(O···O)	2.9127	2.9061	2.9319

[a]Changes relative to monomer given in parentheses.

constants can be a substantial investment for a method such as CCSD(T). Recent experimental success[47−53] in the formation and spectroscopic characterization of noncovalent clusters provides an excellent opportunity to benchmark ab initio methods against experimentally measured properties.

Theoretical studies of the vibrational spectra of hydrogen-bonded clusters often focus on the X−H stretching region, with particular interest in the shift to lower energy (commonly referred to as a "red shift") associated with the donor X−H bond lengthening upon hydrogen bond formation. For water clusters, harmonic vibrational frequency computations indicate that the MP2 method overestimates the shift of the donor O−H stretch to lower energy, relative to CCSD(T) harmonic values and experiment.[54] A proper comparison between calculated and experimental vibrational spectra requires an appropriate anharmonic treatment of the vibrational modes, such as Rayleigh−Schrödinger vibrational second-order perturbation theory (VPT2).[55−58] For the water dimer, Kjaergaard and collaborators[59−65] have improved on the usual double harmonic approximation to probe the O−H stretching region with a variety of impressive techniques, using reduced dimensionality approaches such as local modes (HCAO) and numerically solving a 1-dimensional vibrational Schrödinger equation for the donor O−H stretch, in addition to anharmonic treatments of the complete set of water dimer normal modes through perturbative approaches VPT2 and cc-VSCF with high-accuracy QM methods including CCSD(T). Cremer and co-workers have also investigated the $(H_2O)_2$ spectrum in terms of local and normal mode of vibrations with CCSD(T) calculations and VPT2 corrections.[66] VPT2 gives the exact energy levels of a Morse oscillator and thus is well-suited to describe O−H stretching modes. $(H_2O)_2$ stretching frequencies computed with VPT2 in conjunction with the CCSD(T) method and a triple-ζ basis set compare favorably with experimental values, with a maximum deviation less than 30 cm^{-1} in the fundamental modes.[62]

In addition to the water dimer, the HF dimer is a useful hydrogen-bonding model for pursuing near-CBS vibrational frequencies with correlated QM methods. The structure of this dimer is similar to $(H_2O)_2$, possessing C_s point group symmetry where all atoms are contained in the mirror plane. $(HF)_2$ has been the subject of a number of ab initio investigations.[6,12,67−82] Accurate semiempirical and ab initio potentials[83−87] have been developed from QM calculations and $(HF)_2$ experimental spectra.

In this work, we address the issue of basis set convergence of harmonic vibrational frequencies in these two hydrogen-bonded dimers with a systematic approach toward the CBS limit with wave function methods MP2, CCSD, and CCSD(T). We also make direct comparison to experimental spectra with VPT2 computations.

2. THEORETICAL METHODS

Fully optimized geometries were obtained to compute harmonic and anharmonic vibrational frequencies, utilizing analytic first and second geometrical derivatives. Coupled-cluster and MP2 computations were performed with CFOUR[88] and Gaussian 09,[89] respectively. Anharmonic frequencies were computed within the VPT2 method by double-sided numerical differentiation of analytic second derivatives along normal modes.[90] To examine the basis set convergence of the harmonic vibrational frequencies, we employed the correlation-consistent family of basis sets.[91] In particular, we used the cc-pVXZ (X = D−6, i.e., D,T,Q,5,6) basis sets, as well as the fully augmented aug-cc-pVXZ (aXZ) and "heavy-augmented" versions (haXZ), where diffuse functions were only added to the heavy (i.e., non-hydrogen) atoms. MP2 optimized geometries and harmonic vibrational frequencies were also calculated on a counterpoise-corrected potential energy surface for each basis set to firmly establish CBS estimates and to compare the convergence of the CP-corrected values to those obtained from the standard uncorrected potential energy surfaces. Spherical harmonic *d*, *f*, *g*, *h*, and *i* functions were used instead of their Cartesian counterparts. All calculations were performed with the "frozen core" approximation (i.e., core electrons were not correlated in post-HF computations). CCSD(T)/ha5Z harmonic frequencies of $(H_2O)_2$ were not calculated analytically. Instead, these frequencies were evaluated by 3-point numerical differentiation of energies computed with Molpro[92] at displaced geometries generated by PSI4.[93] The accuracy of this approach was calibrated using the smaller basis sets, for which CCSD(T) analytic second derivative computations were feasible. Harmonic frequencies computed via this finite difference procedure never differed from the analytic values by more than 1 cm^{-1}. Note that minor modification of the CFOUR source code is required to obtain the correct D_0 values with the VPT2 method, as pointed out by the authors in the CFOUR mailing list.[94]

3. RESULTS AND DISCUSSION

3.1. Geometries. Table 1 reports key distances for each monomer and dimer system. The covalent bond lengths are tabulated for the CCSD(T), MP2, and CCSD methods computed with the ha5Z basis set, along with the O···O distance for $(H_2O)_2$ and the F···F distances for $(HF)_2$. Of particular interest in this study are the changes in the OH and

dx.doi.org/10.1021/ct500860v | J. Chem. Theory Comput. 2014, 10, 5426−5435

FH bond lengths when donating a hydrogen bond. Changes relative to the monomer are given in parentheses in Table 1, along with the unique FH and OH covalent bond lengths in the dimers. Relative to CCSD(T), MP2 slightly overestimates the distortion of the covalent bonds when the hydrogen bond is formed, whereas the CCSD method does the opposite. The CCSD method overestimates the distance between the heavy atoms in both dimers relative to CCSD(T) values. The MP2/ha5Z $(HF)_2$ geometry predicts a slightly longer F···F separation relative to CCSD(T), while the $(H_2O)_2$ O···O distance is slightly shorter at the MP2 level. The CCSD(T)/ha5Z geometries here are in excellent agreement with previous benchmark calculations,[37,39,82,95] with maximum deviations from previous CCSD(T) CBS estimates on the order of 0.005 Å for the heavy atom distances, and the agreement improves by an order of magnitude for the intramonomer distances. Cartesian coordinates are provided in the Supporting Information.

3.2. Basis Set Convergence of MP2 Harmonic Vibrational Frequencies. *3.2.1. Estimated MP2 CBS Limit.* The MP2 CBS estimate of each harmonic vibrational frequency in both the monomers and dimers is listed in Table 2. For each normal mode, the MP2 CBS estimate was calculated as the mean of the MP2/a6Z and MP2/ha6Z frequencies. For the dimers, these two values were averaged along with their counterpoise-corrected counterparts (CP-MP2/a6Z and CP-MP2/ha6Z) for the CBS limit estimate (4 values altogether).

Table 2. CBS Limit MP2 Harmonic Vibrational Frequencies (in cm^{-1}) of $(HF)_2$ and $(H_2O)_2$, Along with MP2 and CCSD(T) Values Obtained with the ha5Z Basis Set

	mode	MP2 CBS est.[a]	max abs. dev.[b]	MP2 ha5Z	CCSD(T) ha5Z
HF	ν_1	4136	0	4137	4143
H_2O	ν_2 (a_1)	1631	0	1632	1650
	ν_1 (a_1)	3842	0	3843	3835
	ν_3 (b_2)	3969	0	3970	3945
$(HF)_2$	ν_5 (a')	159	2	160	161
	ν_4 (a')	216	2	217	217
	ν_6 (a'')	463	5	465	461
	ν_3 (a')	566	4	568	566
	ν_2 (a')	4001	1	4002	4026
	ν_1 (a')	4094	0	4095	4105
	$\Delta\nu(FH_d)$	−135	1	−135	−117
$(H_2O)_2$	ν_{12} (a'')	121	1	123	125
	ν_{11} (a'')	145	2	146	142
	ν_8 (a')	149	1	150	148
	ν_7 (a')	184	1	184	185
	ν_6 (a')	351	1	352	351
	ν_{10}(a'')	621	2	624	614
	ν_5 (a')	1632	0	1633	1650
	ν_4 (a')	1651	0	1652	1670
	ν_3 (a')	3738	1	3738	3754
	ν_2 (a')	3834	0	3835	3830
	ν_1 (a')	3937	0	3937	3917
	ν_9 (a'')	3957	0	3957	3936
	$\Delta\nu(OH_d)$	−105	1	−105	81

[a]Mean of the MP2/ha6Z, CP-MP2/ha6Z, MP2/a6Z and CP-MP2/a6Z values for dimers and mean of the MP2/ha6Z and MP2/a6Z values for monomers. [b]Maximum absolute deviation of the 2 monomer or 4 dimer values used to estimate the MP2 CBS limit from their mean.

Even though the fully augmented a6Z basis set has more basis functions, we include the ha6Z frequencies in the CBS estimates because these selectively augmented basis sets tend to provide interaction energies and geometries closer to the CBS limit for hydrogen-bonded clusters.[95,96] For each normal mode, Table 2 also shows the maximum absolute deviation of the MP2/a6Z, MP2/ha6Z, CP-MP2/a6Z, and CP-MP2/ha6Z frequencies from the corresponding CBS estimate. For the HF and H_2O monomer modes, the MP2/ha6Z and a6Z harmonic frequencies agree to within 1 cm^{-1}. In the dimers, the MP2/ha6Z, MP2/a6Z and CP-corrected frequencies are, on average, within 2 cm^{-1} of the CBS estimate for $(HF)_2$ and 1 cm^{-1} for $(H_2O)_2$.

3.2.2. HF and H_2O Monomer Modes. The basis-set convergence of the MP2 harmonic frequencies toward the CBS limit is illustrated in Figures 2−4. For each normal mode,

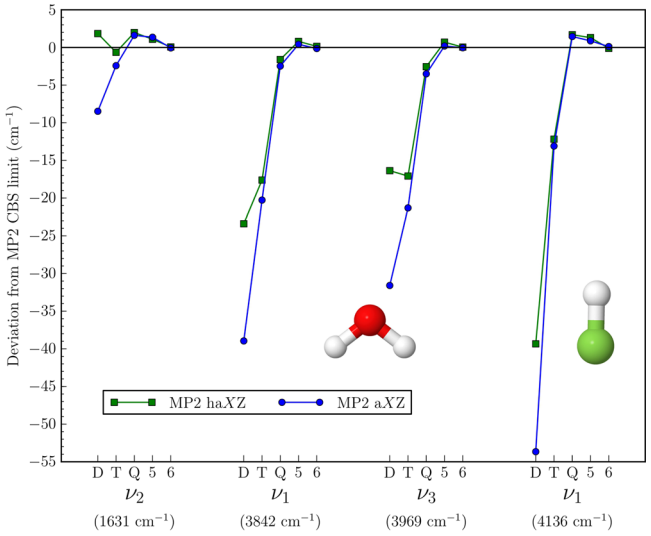

Figure 2. Basis set convergence of MP2 harmonic vibrational frequencies of HF (far right) and H_2O monomers depicted as deviations from the estimated CBS limit (in parentheses).

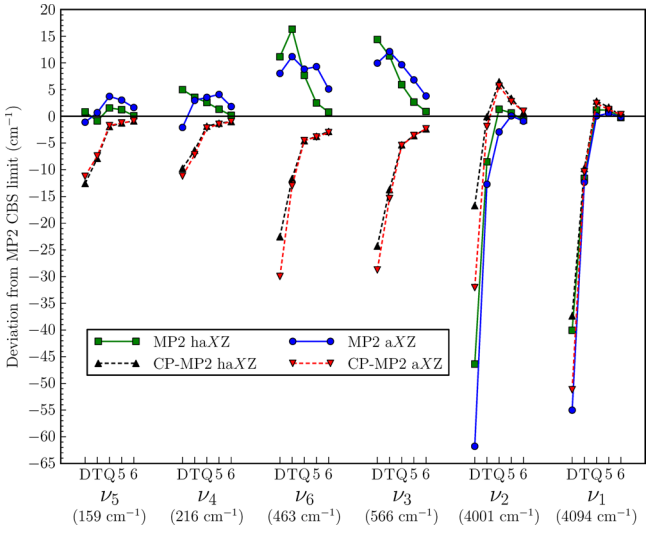

Figure 3. Basis set convergence of MP2 harmonic vibrational frequencies of $(HF)_2$ depicted as deviations from the estimated CBS limit (in parentheses).

dx.doi.org/10.1021/ct500860v | J. Chem. Theory Comput. 2014, 10, 5426−5435

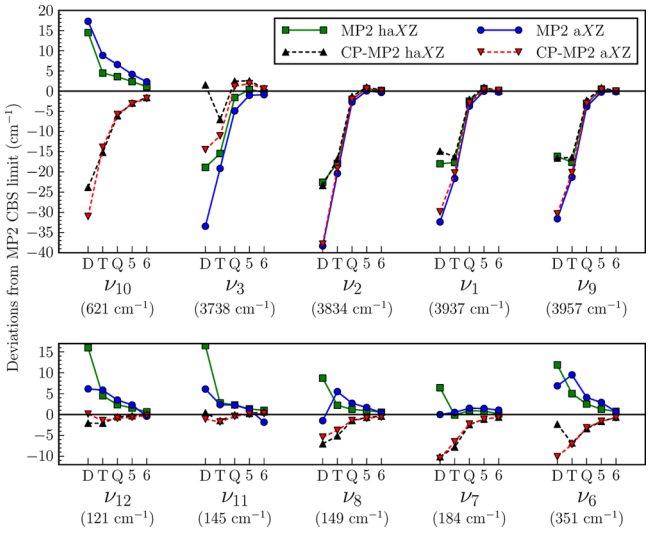

Figure 4. Basis set convergence of MP2 harmonic vibrational frequencies of $(H_2O)_2$ depicted as deviations from the estimated CBS limit (in parentheses).

the MP2 a*XZ* and ha*XZ* deviations from the MP2 CBS limit estimates are plotted across the D−6 progression, marked by circles and squares connected by solid lines, respectively. For the dimers, the corresponding CP-corrected deviations are shown as triangles with dotted lines. Under the label for each normal mode, the MP2 CBS values are given in parentheses.

Figure 2 illustrates the MP2 basis set convergence in the H_2O and HF monomer harmonic vibrational frequencies. The water bend (ν_2) converges quickly, as the MP2/haDZ ν_2 frequency is within 2 cm^{-1} of the MP2 CBS estimate. The HF and OH stretching frequencies converge much more slowly. The MP2/aDZ values underestimate the corresponding CBS frequencies by more than 30 cm^{-1} in each stretching mode. Increasing the basis set to haTZ or aTZ improves the predicted MP2 stretching frequencies to within ca. 10−20 cm^{-1}. Agreement to within 5 cm^{-1} of the MP2 CBS limit is achieved with quadruple-ζ basis sets for each mode.

3.2.3. $(HF)_2$ and $(H_2O)_2$ Intermonomer Modes. There are four intermonomer modes in the HF dimer (ν_5, ν_4, ν_6, and ν_3) and six in $(H_2O)_2$ (ν_{12}, ν_{11}, ν_8, ν_7, ν_6, and ν_{10}). See refs 62 and 87 or Tables S7 and S13 in the Supporting Information for a description of each of these intermonomer normal modes. As can be seen in Figures 3 and 4, the basis-set convergence of the intermonomer frequencies toward the MP2 CBS limit is very similar in both complexes. For both dimers, the slowest basis-set convergence for the MP2 harmonic frequencies is seen in the 2 highest-frequency intermonomer modes ca. 350−650 cm^{-1} (ν_6 and ν_3 for $(HF)_2$ and ν_6 and ν_{10} for $(H_2O)_2$). In each complex, these 2 modes consist of one in-plane (a') and one out-of-plane (a'') bending motion of the X—H···X angle associated with the donor hydrogen involved in the H-bond. Although MP2 frequencies computed with triple-ζ basis sets are within 10 cm^{-1} for the lowest-energy intermonomer modes (<250 cm^{-1}), basis sets of at least quadruple-ζ quality are required to be within 10 $cm^{-1}$of the MP2 CBS limit for the more challenging higher-energy intermonomer modes above 350 cm^{-1}. We note that the energetic ordering of the nearby modes ν_{11} (a'') and ν_8 (a') in $(H_2O)_2$ is reversed in the harmonic frequencies computed using the double-ζ basis sets, with the exception of CP-MP2/aDZ.

The CP-corrected and uncorrected values tend to converge from opposite sides of the CBS limit, reminiscent of the convergence of interaction energies.[96] The net effects of the CP procedure, however, are somewhat mixed. In $(H_2O)_2$, for example, the lowest-energy frequencies (ν_{12}, ν_{11}, and ν_8) computed with smaller basis sets are usually shifted closer to the MP2 CBS limit when the procedure is applied, particularly for MP2/haDZ frequencies. In contrast, the CP procedure increases the deviations from the CBS limit for the lowest-frequency modes in $(HF)_2$ (ν_5 and ν_4).

The largest differences in MP2 and CP-MP2 intermonomer frequencies are observed for the two highest-frequency intermonomer modes (ca. 350−650 cm^{-1}) in each dimer. Even with the large a6Z basis set, the difference between CP corrected and uncorrected frequencies for $(HF)_2$ grows as large as 8 cm^{-1} for ν_6 and 6 cm^{-1} for ν_3. In $(H_2O)_2$, the largest difference between MP2/a6Z and CP-MP2/a6Z frequencies also occurs in the out-of-plane bending mode (4 cm^{-1} for ν_{10}).

3.2.4. $(HF)_2$ and $(H_2O)_2$ Intramonomer Modes. The basis-set dependence of the intramonomer frequencies in these dimers closely follows what was seen for the isolated monomers in Figure 2 at the MP2 level of theory. The harmonic frequencies of the bending modes in the water dimer are within 10 cm^{-1} of the MP2 CBS estimate with the double-ζ basis sets and within 5 cm^{-1} with the triple- ζ basis sets. The two bending modes in $(H_2O)_2$ are excluded from Figure 4 due to this rapid convergence, but the data can be found in the Supporting Information.

The intramonomer stretching frequencies are underestimated with the smaller basis sets, by more than 60 cm^{-1} for FH donor stretch and 38 cm^{-1} for the symmetric OH acceptor stretch computed with the aDZ basis set. As with the monomers, the quadruple-ζ basis sets are needed to obtain OH and FH stretching frequencies within 5 cm^{-1} of the MP2 CBS limit.

The "red-shifted" donor hydrogen stretches (ν_2 in $(HF)_2$ and ν_3 in $(H_2O)_2$) are affected by the CP procedure much more than the other intramonomer FH and OH stretching modes not directly participating in the hydrogen bond. As shown in Figure 3 for $(HF)_2$, the CP procedure hardly affects the MP2 frequency of ν_1, regardless of the basis set. The maximum shift caused by the CP procedure for this free FH stretch in any basis set is less than 4 cm^{-1}. For the donor FH stretch ν_2, on the other hand, the MP2 and CP-MP2 frequencies differ by nearly 30 cm^{-1} with the aDZ and haDZ basis sets. A similar trend is observed for the OH stretches in $(H_2O)_2$. The CP procedure only noticeably affects the OH donor stretch (ν_3), improving the haDZ and aDZ frequencies by roughly 15 cm^{-1} relative to the MP2 CBS limit.

Although the CP procedure tends to move the double and triple-ζ donor stretching frequencies (ν_2 in $(HF)_2$ and ν_3 in $(H_2O)_2$) closer to the MP2 CBS limit, it leads to an appreciable underestimation of the shift to lower energy of these modes relative to the monomer stretching frequencies $\Delta\nu(FH_d)$ (and $\Delta\nu(OH_d)$ in Table 2). The calculated CP-MP2 double-ζ and triple-ζ values underestimate the CBS shift by more than 20 and 10 cm^{-1}, respectively. The $\Delta\nu(FH_d)$ values from the standard MP2 frequencies are within 8 and 4 cm^{-1} with these basis sets. The same pattern can be seen for the $\Delta\nu(OH_d)$ in $(H_2O)_2$ as well.

3.3. Comparison of Harmonic MP2 and CCSD(T) Frequencies. Because CCSD(T) harmonic frequency computations with sextuple-ζ basis sets were infeasible, the

dx.doi.org/10.1021/ct500860v | J. Chem. Theory Comput. 2014, 10, 5426−5435

comparison between MP2 and CCSD(T) frequencies utilizes results obtained with the ha5Z basis set. The MP2/ha5Z harmonic frequencies in the penultimate column of Table 2 are within a few cm^{-1} of the MP2 CBS limit. Even though the effects of the CP procedure will not be identical for the MP2 and CCSD(T) methods, the CCSD(T)/ha5Z harmonic frequencies in the last column of Table 2 are expected to lie close to the CCSD(T) CBS limit.

For the HF monomer stretch listed first in Table 2, the MP2 value agrees well with the CCSD(T) result, underestimating the harmonic frequency by 6 cm^{-1}. However, the MP2/ha5Z H_2O monomer harmonic frequencies show larger deviations from the corresponding CCSD(T)/ha5Z values. MP2 underestimates the bending mode (ν_2) by 18 cm^{-1} but overestimates both of the stretching frequencies (by as much as 25 cm^{-1} for ν_3).

Comparing the $(HF)_2$ and $(H_2O)_2$ CCSD(T) and MP2 intermonomer modes, the MP2 frequency values are in excellent agreement with CCSD(T). Only ν_{10} in $(H_2O)_2$ differs by 10 or more cm^{-1} between the methods. The average absolute deviation between MP2 and CCSD(T) intermonomer frequencies is only 3 cm^{-1} with the ha5Z basis set for all 10 intermonomer modes (ν_5, ν_4, ν_6, and ν_3 for $(HF)_2$ and ν_{12}, ν_{11}, ν_8, ν_7, ν_6, and ν_{10} for $(H_2O)_2$).

For the intramonomer bending and stretching modes, much larger discrepancies are observed between MP2/ha5Z and CCSD(T)/ha5Z harmonic frequencies, and they tend to mimic the differences seen for the isolated monomers. MP2 consistently overestimates the free OH stretches relative to CCSD(T). The discrepancy is as small as 5 cm^{-1} for the symmetric acceptor OH stretch (ν_2), and it is large as 20−21 cm^{-1} for the two highest-frequency OH stretching modes in $(H_2O)_2$ (ν_9 and ν_1). For the HOH bending modes in $(H_2O)_2$, the MP2/ha5Z harmonic frequencies are always smaller by 17−18 cm^{-1} than the CCSD(T) results, just like the monomer. In $(HF)_2$, the MP2 computations underestimate the free FH stretch by 10 cm^{-1}, while the bound FH stretch is underestimated by 24 cm^{-1} relative to CCSD(T).

The last row in Table 2 for each dimer gives the shift of the donor stretching mode relative to the monomer stretch, denoted $\Delta\nu(FH_d)$ and $\Delta\nu(OH_d)$, computed at the same level of theory (symmetric OH stretch in the case of H_2O). A negative value for $\Delta\nu$ implies a shift to lower energy (a.k.a. a red-shift). The magnitude of the shift is overestimated in both dimer systems at the MP2 level. The overestimation is more severe in the water dimer (−105 cm^{-1} vs −81 cm^{-1} at the MP2 and CCSD(T) levels, respectively). Recall the XH bond lengthening (Table 1) associated with hydrogen bond formation (and the red-shifted XH stretching mode) is also larger at the MP2 level for each dimer complex here, as discussed in Section 3.1.

4. ANHARMONIC VIBRATIONAL FREQUENCIES AND DISSOCIATION ENERGIES

Tables 3−6 summarize the VPT2 frequencies of the HF and H_2O monomers and dimers computed with CCSD(T), MP2 and CCSD methods and the haQZ basis set. The VPT2 results for each electron correlation method are given as deviations from the experimental values, where the sign convention is such that a positive value implies an overestimated frequency relative to the experimental reference. For the reference values, gas-phase values are given when possible.

Table 3. Deviations between VPT2 Fundamental Transition Energies and Experimental Vibrational Frequencies of HF and $(HF)_2$ and Dissociation Energy (D_0) (in cm^{-1}) of $(HF)_2$ Computed with CCSD(T), MP2, and CCSD Methods with the haQZ Basis Set

		exp	CCSD(T)	MP2	CCSD
HF	ν_1	3961[a]	+2	+1	+52
$(HF)_2$	ν_5 (a')	125[b]	+7	+6	+4
	ν_4 (a')	161[c]	+11	+11	+3
	ν_6 (a'')	380[d]	+9	+23	+7
	ν_3 (a')	475[e]	−22	−14	−34
	ν_2 (a')	3868[f]	+1	−17	+65
	ν_1 (a')	3931[f]	−1	−7	+51
	$\Delta\nu(FH_d)$	−93[f]	−1	−18	+13
	D_0	1062[g]	−2	−24	−60

[a]Ref 97 (gas). [b]Ref 87 (gas). [c]Ref 86 (gas). [d]Ref 99 (gas). [e]Ref 100 (gas). [f]Ref 101 (gas). [g]Ref 102 (gas).

Table 4. Select VPT2 Overtone and Combination Levels (in cm^{-1}) of HF and $(HF)_2$ Computed with MP2, CCSD, and CCSD(T) Methods with the haQZ Basis Set

		exp	CCSD(T)	MP2	CCSD
HF	$2\nu_1$	7751[a]	−4	−2	+98
$(HF)_2$	$2\nu_2$	7550[b]	0	−39	+136
	$2\nu_1$	7683[c]	+8	−2	+117
	$\nu_2+\nu_5$	4001[d]	+5	−12	+65
	$\nu_2+\nu_4$	4049[d]	+6	−8	+63
	$\nu_1+\nu_5$	4058[d]	+4	−2	+53
	$\nu_1+\nu_4$	4099[d]	+3	−2	+48
	$\nu_1+\nu_3$	4418[e]	−27	−24	+13

[a]Ref 97 (gas). [b]Ref 104 (gas). [c]Ref 105 (gas). [d]Ref 103 (gas). [e]Ref 101 (gas).

Table 5. Deviations between VPT2 Fundamental Transition Energies and Experimental Vibrational Frequencies and Dissociation Energy (D_0) (in cm^{-1}) of $(H_2O)_2$ Computed with CCSD(T), MP2, and CCSD Methods with the haQZ Basis Set

		exp	CCSD(T)	MP2	CCSD
H_2O	ν_2	1595[a]	+3	−14	+18
	ν_1	3657[a]	−2	+12	+46
	ν_3	3756[a]	−6	+27	+38
$(H_2O)_2$	ν_{12}	88[b]	−9	−16	−26
	ν_{11}	108[b]	+3	+39	−6
	ν_8	103[b]	0	0	0
	ν_7	143[c]	0	−1	−5
	ν_6	311[d]	−18	−27	−25
	ν_{10}	523[d]	−28	−18	−50
	ν_5	1599[d]	0	−10	+25
	ν_4	1616[d]	0	−21	+14
	ν_3	3602[e]	+3	−6	+61
	ν_2	3651[e]	−1	+15	+47
	ν_1	3730[e]	−3	+37	+47
	ν_9	3745[e]	+2	+14	+48
	$\Delta\nu(OH_d)$	−55[e]	+6	−18	+15
	D_0	1105[f]	−21	−2	−81

[a]HITRAN 2006 values from ref 62. [b]Ref 107 (gas). [c]Ref 108 (gas). [d]Ref 109 (Ne matrix). [e]Ref 52 (gas). [f]Ref 110 (gas).

4.1. Monomers. The first row of data in Table 3 compares the experimental HF stretching fundamental to VPT2 results.

dx.doi.org/10.1021/ct500860v | J. Chem. Theory Comput. 2014, 10, 5426−5435

Table 6. Select VPT2 Overtone and Combination Levels (in cm^{-1}) of $(H_2O)_2$ Computed with MP2, CCSD, and CCSD(T) Methods with the haQZ Basis Set

		exp	CCSD(T)	MP2	CCSD
H_2O	$2\nu_2$	3152[a]	+10	−23	+38
	$2\nu_1$	7202[a]	+21	+52	+122
	$2\nu_3$	7445[a]	−43	+27	+46
	$\nu_1+\nu_2$	5235[a]	+2	−2	+66
	$\nu_2+\nu_3$	5331[a]	−3	+12	+56
	$\nu_1+\nu_3$	7250[a]	−11	+43	+85
$(H_2O)_2$	$2\nu_5$	3163[b]	+5	−14	+53
	$2\nu_4$	3194[b]	+3	−37	+31
	$2\nu_3$	7018[b]	+46	+17	+172
	$2\nu_2$	7193[c]	+24	+57	+122
	$2\nu_1$	7362[b]	−49	+34	+56
	$2\nu_9$	7442[b]	−44	−18	+50
	$\nu_3+\nu_4$	5219[d]	−10	−41	+63
	$\nu_2+\nu_5$	5243[b]	−9	−5	+66
	$\nu_9+\nu_5$	5329[d]	−3	+4	+69
	$\nu_1+\nu_4$	5345[d]	−19	+1	+46
	$\nu_1+\nu_3$	7240[c]	+18	+57	+123
	$\nu_9+\nu_2$	7250[c]	−17	+17	+80

[a]HITRAN 2006 values from ref 62. [b]Ref 109 (Ne matrix). [c]Ref 113 (gas). [d]Ref 114 (gas).

The CCSD(T) and MP2 values computed with the haQZ basis set are in excellent with the experimental value of 3961 cm^{-1}, each within 2 cm^{-1} of the reference. The CCSD method overestimates the ν_1 position by more than 50 cm^{-1}. For the first overtone of the HF stretch in Table 4, the absolute deviation from experiment approximately doubles for each method, as the CCSD(T) and MP2 $2\nu_1$ positions are within 4 and 2 cm^{-1} of the experimental spectrum, respectively.

The H_2O VPT2 fundamental frequencies are shown in the first rows of Table 5. For the 3 normal modes, the CCSD(T)/haQZ values are much closer to experiment than the MP2 predicted frequencies. The largest deviation with the CCSD(T) method is only a 6 cm^{-1} underestimation of the antisymmetric OH stretch ν_3. As with the harmonic vibrational frequencies, the MP2 method predicts OH stretching frequencies too high, compared to CCSD(T) calculations, while the bending mode ν_2 is predicted too low at the MP2/haQZ level. The CCSD/haQZ fundamentals are the farthest from experiment, with the frequencies of the OH stretching modes overestimated by more than 40 cm^{-1} on average.

The first overtones and combination bands of the H_2O vibrational modes are shown in Table 6. For the first bending overtone ($2\nu_2$) and the combination bands involving the bending mode ($\nu_1+\nu_2$ and $\nu_2+\nu_3$), the CCSD(T)/haQZ VPT2 results are again in good agreement with experiment. $2\nu_2$ is within 10 cm^{-1} of experiment, while the two combinations bands only deviate by 2 and 3 cm^{-1}. Because the MP2 method overestimates the fundamental stretching frequencies and underestimates the H_2O bending frequency, rather good agreement is obtained for the combination bands between 5200 and 5350 cm^{-1} due to a rather favorable cancellation of errors. For example, MP2 underestimates the bending mode ν_2 by −14 cm^{-1} and overestimates the symmetric OH stretch ν_1 by +12 cm^{-1}, and the deviation from the experimental value of the combination band $\nu_1+\nu_2$ is −2 cm^{-1}.

The first OH stretching overtones in H_2O calculated with CCSD(T) show much larger deviations relative to experiment. This is due to strong Darling−Dennison resonance,[98] which is unaccounted for in the standard VPT2 implementation used here. An approach such as that undertaken in ref 98 would shift the CCSD(T) $2\nu_1$ and $2\nu_3$ values closer to the experiment. The OH stretching combination band $\nu_1+\nu_3$ is unaffected by this resonance, and the CCSD(T)/haQZ frequency of 7239 cm^{-1} is in good agreement with the measured value of 7250 cm^{-1}. The MP2 and CCSD methods overestimate the energy of the $\nu_1+\nu_3$ transition by more than 40 and 80 cm^{-1}, respectively.

4.2. $(HF)_2$. Table 3 compares VPT2 fundamental frequencies of $(HF)_2$ computed with CCSD(T), MP2, and CCSD using the haQZ basis set to experimental results.[86,87,99−105] Note, however, that the experimental values for the lowest-energy transitions are actually indirect estimates.[86,87,99,100] The largest deviations from the experimental values occur for the same intermonomer modes that exhibited the slowest convergence to the MP2 CBS limit (ν_6 and ν_3 in Figure 3). MP2 overestimates the ν_6 fundamental by +23 cm^{-1} whereas CCSD and CCSD(T) underestimate ν_3 by −34 cm^{-1} and −22 cm^{-1}, respectively.

In contrast to the monomer, the CCSD(T)/haQZ VPT2 intramonomer frequencies of $(HF)_2$ are in far better agreement with experiment than MP2/haQZ values. The CCSD(T) calculated FH stretching fundamentals are within 1 cm^{-1} of the experimental values, and the $\Delta\nu(FH_d)$ is within 1 cm^{-1} as well. MP2 underestimates both HF stretching fundamental frequencies by −7 cm^{-1} and −17 cm^{-1} for FH_f and FH_d stretches, respectively. In contrast, the CCSD method overestimates these stretching modes by +51 cm^{-1} for ν_1 and +65 cm^{-1} for ν_2.

In the last row of Table 3, the calculated D_0 values are compared to the experimental value of 1062 cm^{-1}.[102] The CCSD(T) D_0 is within 2 cm^{-1} of this reference value. Although this remarkable level of agreement is somewhat fortuitous, it can be understood in light of the recent work of Řezáč et al.[82] They have computed the dissociation energy of the HF dimer with a series of high-level ab initio calculations, including full quadruple excitations via CCSDTQ, relativistic effects and a diagonal Born−Oppenheimer correction. They concluded that the sum of those corrections to D_0 amounts to less than 2 cm^{-1}. That work also computed CCSD(T) VPT2 frequencies with the fully augmented aug-cc-pVQZ basis set, which overall agree with those computed here. The only substantial differences between the two calculations occur in the intermonomer modes, where ν_6 is shifted 20 cm^{-1} higher with the aug-cc-pVQZ basis set. However, the computed frequencies for ν_6 have been shown to be extremely sensitive to small changes in the basis set.[80]

Vibrational overtone and combination band transition energies for the HF dimer are presented in Table 4. For this dimer, the CCSD(T) VPT2 energy levels predict the $2\nu_1$ and $2\nu_2$ transitions to within 8 cm^{-1} of experiment. The first overtone of the donor FH stretch observed at 7550 cm^{-1} is perfectly matched at the CCSD(T)/haQZ level. The combination bands in the 4000−4100 cm^{-1} range, corresponding to excitations in one HF stretching mode and one intermonomer mode, are also captured very well by the CCSD(T) method, with a maximum absolute deviation from experiment of only 6 cm^{-1}. The combination band involving ν_3 in the last row reveals larger discrepancies, although only slightly more than the deviation seen for the ν_3 fundamental in Table 3. With the exception of the $2\nu_2$ transition predicted 39 cm^{-1} too low, the MP2 overtones and combination bands are also rather close to the experimental values. The CCSD method consistently overestimates the stretching overtones and

dx.doi.org/10.1021/ct500860v | J. Chem. Theory Comput. 2014, 10, 5426−5435

combination bands, by more than 100 cm^{-1} in the case of $2\nu_2$ and $2\nu_1$.

4.3. $(H_2O)_2$. Table 5 compares VPT2 fundamental frequencies of $(H_2O)_2$ computed with CCSD(T), MP2, and CCSD using the haQZ basis set to experimental results.[52,106−110] Note that experimental values for $(H_2O)_2$ vibrational frequencies can vary by several cm^{-1} due to differing experimental conditions. For example, the rotational temperatures have been estimated to be around 5K for gas-phase measurements of the intermonomer fundamentals,[107,108] but the vibrational degrees of freedom "may have different effective temperatures or even non-thermal distributions"[52] depending on the expansion conditions. Refs 61 and 106 provide thorough reviews of the various experimental vibrational frequencies that can be found in the literature. Also note that several $(H_2O)_2$ vibrational transitions have only been measured in Ne matrix environments, where interactions with the dimer shift $(H_2O)_2$ fundamentals by as much as 20% relative to gas-phase values.[109,111] Lastly, the relatively large tunneling splittings[112] in $(H_2O)_2$ are unaccounted for in the VPT2 calculations.

As with $(HF)_2$, the CCSD(T) fundamental vibrational energies of $(H_2O)_2$ tend to agree quite well with the measured transitions (column 3 of Table 5). For the four lowest-energy vibrations, the CCSD(T) results show a maximum deviation from experiment of −9 cm^{-1} (ν_{12}) and an average absolute deviation around 3 cm^{-1}. For the MP2 and CCSD VPT2 frequencies (last two columns in Table 5), the maximum deviations in these four modes are appreciably larger at +39 cm^{-1} and −26 cm^{-1}, respectively (ν_{11} and ν_{12}).

The two highest-energy intermonomer vibrations (ν_6 and ν_{10}) are particularly challenging. Although all three methods consistently underestimate these frequencies with respect to experiment, none of them reproduce either of the experimental ν_6 or ν_{10} frequencies to within 17 cm^{-1}. This results is perhaps not too surprising in light of the slow basis set convergence exhibited by the MP2 harmonic frequencies for these two modes as discussed in Section 3.2.3.

Looking at the intramonomer fundamental frequencies near the bottom of Table 5, the CCSD(T) VPT2 transitions for these six modes show remarkable agreement with the experimental values. All of the OH-stretching fundamental transitions computed with CCSD(T) are within ±3 cm^{-1} of the gas-phase positions, with $\Delta\nu(OH_d)$ within 6 cm^{-1} of experiment. Deviations from experimental intramonomer vibrational frequencies are significantly larger for the VPT2 results computed with the MP2 and CCSD methods, as with the H_2O monomer. The average absolute deviation in the six intramonomer modes is 17 cm^{-1} with MP2 and 41 cm^{-1} with CCSD. MP2 overestimates the shift associated with the donor stretching mode ($\Delta\nu(OH_d)$) by nearly 20 cm^{-1}, whereas CCSD underestimates the shift by −15 cm^{-1}. These deviations are nearly identical to those seen for the harmonic frequencies in Table 2. It is interesting to note that the order of the two highest-energy MP2 stretching frequencies changes with the anharmonic corrections. This reordering also occurs for VPT2 frequencies computed with the haDZ and haTZ basis sets (see Supporting Information).

D_0 values computed with each correlated method are given in the last row of Table 5. The D_0 values computed with CCSD(T) and MP2 methods compare fairly well with the experimental value[110] of 1105 cm^{-1} (−21 cm^{-1} and −2 cm^{-1}, respectively). With the haQZ basis set, the CCSD(T) electronic dissociation energy (D_e) of 1752 cm^{-1} is slightly larger than the estimated CCSD(T) CBS limit (within the frozen core approximation). With the ha5Z basis set, the CCSD(T) D_e computed here is reduced to 1745 cm^{-1}, in good agreement with the CCSD(T) CBS estimate of 1743 cm^{-1} obtained by Lane[37] utilizing geometries near the CCSD(T) CBS limit. The MP2 D_e values obtained in the present study with the haQZ and ha5Z basis sets are 1747 and 1740 cm^{-1}, respectively. Despite the much larger errors for MP2/haQZ fundamental frequencies, some favorable error cancellation leads to an MP2/haQZ D_0 that is within 2 cm^{-1} of the experimental value.

The bottom part of Table 6 shows $(H_2O)_2$ combination band and overtone transition frequencies for which experimental data[109,113,114] is available for comparison. The CCSD(T) bending overtones ($2\nu_5$ and $2\nu_4$) are within 5 cm^{-1} of the experimental positions.[109] However, the stretching overtones ($2\nu_3$, $2\nu_2$, $2\nu_1$, and $2\nu_9$) show much larger deviations at the CCSD(T) level. As discussed for the H_2O monomer overtones in Section 4.1, a Darling−Dennison resonance is the origin of these large discrepancies.[98]

The VPT2 transition energies of the intramonomer combination bands are shown near the bottom of Table 6. The CCSD(T) transitions involving the bending modes between 5200 and 5400 cm^{-1} compare favorably with experiment, underestimating the energy of each transition by a maximum of 20 cm^{-1} and less than 10 cm^{-1} on average. CCSD(T)/haQZ VPT2 results for the stretching combination bands in the last two rows of Table 5 are in better agreement with experiment than the stretching overtones, reproducing the experimental values to within 20 cm^{-1}. The performance of MP2 for these combination bands is inconsistent. Three of the MP2 transitions are predicted to within 5 cm^{-1} of experiment, while the lowest-energy combination band deviates from the experimental value by −41 cm^{-1}, and the combination band arising from excitations in both donor stretching modes ($\nu_1+\nu_3$) deviates by +60 cm^{-1}.

5. CONCLUSIONS

In this work, we have established benchmark values for the harmonic vibrational frequencies of $(H_2O)_2$ and $(HF)_2$ with correlated wave function methods and large correlation-consistent basis sets. MP2 harmonic vibrational frequencies have been computed with basis sets as large as aug-cc-pV6Z on both standard and counterpoise-corrected potential energy surfaces. In addition, we have calculated anharmonic vibrational frequencies with these correlated methods and the haQZ basis set by way of VPT2 computations. The main conclusions for this investigation are as follows:

i. To obtain harmonic vibrational frequencies that are consistently converged to within 10 cm^{-1} of the CBS limit, a basis set of quadruple-ζ quality is needed according to our analysis at the MP2 level of theory with the haXZ and aXZ families of correlation-consistent basis sets. For these dimers, the haQZ basis set gives frequencies exhibiting average absolute deviations from the MP2 CBS limit of less than 3 cm^{-1}. In particular, the harmonic frequencies of the OH and FH stretching modes are greatly improved with these quadruple-ζ basis sets compared to their triple-ζ counterparts. The maximum absolute errors in the stretching modes decreases from 10−20 cm^{-1} in the haTZ basis set to

1−3 cm^{-1} with the haQZ basis set. Use of the fully augmented aQZ basis set or application of the counterpoise procedure does not improve the MP2/haQZ harmonic frequencies relative to the CBS values in either of the dimers, despite the additional computational effort.

ii. Counterpoise corrections affect the MP2 harmonic vibrational frequencies in different ways, depending on the nature of the normal mode. The standard MP2 harmonic calculations tend to overestimate the frequencies of the intermonomer modes, while the CP corrections tend to result in underestimated intermonomer frequencies. This is similar to the convergence patterns seen for binding energies in hydrogen-bonded dimers.[96] The intramonomer modes are hardly affected by the CP correction, with the exception of the donor stretch. The CP procedure for the double- and triple-ζ basis sets examined here moves the donor stretch frequency position to higher energy and closer to the MP2 CBS estimate. Unfortunately, the net result is an underestimated "red shift" that is farther from the estimated CBS limit.

iii. CCSD(T) anharmonic vibrational frequencies computed with VPT2 and the haQZ basis set show excellent agreement with available experimental values, particularly for the intramonomer fundamental vibrational transitions. The CCSD(T) intramonomer frequencies agree with experiment to within a few cm^{-1} for both the $(HF)_2$ and $(H_2O)_2$ dimers. The low-energy intermonomer fundamental frequencies are predicted well by CCSD(T), typically within 10 cm^{-1}, while the deviations exceed 20 cm^{-1} for the highest-energy intermonomer modes.

iv. The accuracy of the CCSD(T) predicted anharmonic vibrational transitions decreases slightly for the overtones and combination bands. The combination bands and overtones between 3000 and 6000 cm^{-1} are typically within 10 cm^{-1} of experiment, while the deviations can exceed 50 cm^{-1} for the first OH stretching overtones located above 7000 cm^{-1}, calculated within the standard VPT2 implementation.[88] All of the $(HF)_2$ overtones and combination bands agree well with experimental spectra, with no computed transitions differing by more than 20 cm^{-1} from experiment and only one transition differing by more than 8 cm^{-1}.

v. The CCSD(T)/haQZ dissociation energies computed with VPT2 for these dimers agree very well with experiment. The predicted D_0 for $(H_2O)_2$ of 1084 cm^{-1} underestimates the experimental value by only 21 cm^{-1} and that for $(HF)_2$ of 1060 cm^{-1} is only 2 cm^{-1} below experiment. These results demonstrate the accuracy that can be realized for computing vibrational properties of small clusters, using the CCSD(T) method in conjunction with sufficiently large basis sets as well as an appropriate treatment of anharmonic effects with VPT2.

■ ASSOCIATED CONTENT

Supporting Information

Optimized molecular geometries, harmonic vibrational frequencies, VPT2 fundamental frequencies, and zero-point vibrational energies. This material is available free of charge via the Internet at http://pubs.acs.org.

■ AUTHOR INFORMATION

Corresponding Author

*E-mail: tschumpr@olemiss.edu.

Notes

The authors declare no competing financial interest.

■ ACKNOWLEDGMENTS

This material is based upon work supported by the National Science Foundation under Grant Nos. EPS-0903787 and CHE-1156713. The authors also thank the Mississippi Center for Supercomputing Research for providing computational resources.

■ REFERENCES

(1) Pimentel, G. C.; McClellan, A. L. *The Hydrogen Bond*; W.H. Freeman: San Francisco, 1960.
(2) Jeffrey, G. A.; Saenger, W. *Hydrogen Bonding in Biological Structures*; Springer-Verlag: Berlin, 1994.
(3) Stone, A. *The Theory of Intermolecular Forces*; Clarendon: Oxford, 1997.
(4) Morokuma, K.; Pedersen, L. *J. Chem. Phys.* **1968**, *48*, 3275−3282.
(5) Kollman, P. A.; Allen, L. C. *J. Chem. Phys.* **1969**, *51*, 3286−3293.
(6) Kollman, P. A.; Allen, L. C. *J. Chem. Phys.* **1969**, *52*, 5085−5093.
(7) Morokuma, K.; Winick, J. R. *J. Chem. Phys.* **1970**, *52*, 1301−1306.
(8) Hankins, D.; Moskowitz, J.; Stillinger, F. *J. Chem. Phys.* **1970**, *53*, 4544−4554.
(9) Del Bene, J.; Pople, J. *J. Chem. Phys.* **1973**, *52*, 4858−4866.
(10) Del Bene, J. E.; Pople, J. *J. Chem. Phys.* **1973**, *58*, 3605−3608.
(11) Kistenmacher, H.; Lie, G.; Popkie, H.; Clementi, E. *J. Chem. Phys.* **1974**, *61*, 546−561.
(12) Dill, J.; Allen, L.; Topp, W.; Pople, J. *J. Am. Chem. Soc.* **1975**, *97*, 7220−7226.
(13) Burnham, C. J.; Xantheas, S. S. *J. Chem. Phys.* **2002**, *116*, 1500−1510.
(14) Bukowski, R.; Szalewicz, K.; Groenenboom, G. C.; van der Avoird, A. *Science* **2007**, *315*, 1249−1252.
(15) Cencek, W.; Szalewicz, K.; Leforestier, C.; van Harrevelt, R.; van der Avoird, A. *Phys. Chem. Chem. Phys.* **2008**, *10*, 4716−31.
(16) Huang, X.; Braams, B.; Bowman, J. M.; Kelly, R. E. A.; Tennyson, J.; Groenenboom, G. C.; van der Avoird, A. *J. Chem. Phys.* **2008**, *128*, 34312.
(17) Shank, A.; Wang, Y.; Kaledin, A.; Braams, B. J.; Bowman, J. M. *J. Chem. Phys.* **2009**, *130*, 144314.
(18) Wang, Y.; Shepler, B. C.; Braams, B. J.; Bowman, J. M. *J. Chem. Phys.* **2009**, *131*, 54511.
(19) Wang, Y.; Huang, X.; Shepler, B. C.; Braams, B. J.; Bowman, J. M. *J. Chem. Phys.* **2011**, *134*, 94509.
(20) Wang, Y.; Bowman, J. *J. Chem. Phys.* **2011**, *134*, 154510.
(21) Leforestier, C.; Szalewicz, K.; van der Avoird, A. *J. Chem. Phys.* **2012**, *137*, 14305.
(22) Babin, V.; Medders, G. R.; Paesani, F. 2012, *3*, 3765−3769.
(23) Medders, G. R.; Babin, V.; Paesani, F. *J. Chem. Theory Comput.* **2013**, *9*, 1103−1114.
(24) Babin, V.; Medders, G. R.; Paesani, F. *J. Chem. Theory Comput.* **2014**, *10*, 1599−1607.
(25) Clementi, E.; Kołos, W.; Lie, G.; G, R. *Int. J. Quantum Chem.* **1980**, *17*, 377−398.
(26) Koehler, J.; Saenger, W.; Lesyng, B. *J. Comput. Chem.* **1987**, *8*, 1090−1098.
(27) Hermansson, K. *J. Chem. Phys.* **1988**, *89*, 2149−2159.
(28) Mó, O.; Yáñez, M.; Elguero, J. *J. Chem. Phys.* **1992**, *97*, 6628−6638.
(29) Mhin, B. J.; Kim, J.; Lee, S.; Lee, J. Y.; Kim, K. S. *J. Chem. Phys.* **1994**, *100*, 4484−4486.
(30) Xantheas, S. S. *J. Chem. Phys.* **1994**, *100*, 7523−7534.
(31) Hodges, M. P.; Stone, A. J.; Xantheas, S. S. 1997, *101*, 9163−9168.

(32) Karpfen, A. Case Studies in Cooperativity in Hydrogen-Bonded Clusters and Polymers. In *Molecular Interactions: From van der Waals to Strongly Bound Complexes*; Scheiner, S., Ed.; John Wiley and Sons: New York, 1997; Chapter 8, pp 265−296.
(33) Masella, M.; Gresh, N.; Flament, J. *J. Chem. Soc., Faraday Trans.* **1998**, *94*, 2745−2753.
(34) Xantheas, S. S. *Chem. Phys.* **2000**, *258*, 225−231.
(35) Bartlett, R. J. *WIREs Comput. Mol. Sci.* **2012**, *2*, 126−138.
(36) Raghavachari, K.; Trucks, G. W.; Pople, J. A.; Head-Gordon, M. *Chem. Phys. Lett.* **1989**, *157*, 479−483.
(37) Lane, J. R. *J. Chem. Theory Comput.* **2013**, *9*, 316−323.
(38) Řezáč, J.; Hobza, P. *J. Chem. Theory Comput.* **2012**, *9*, 364−369.
(39) Tschumper, G. S.; Leininger, M. L.; Hoffman, B. C.; Valeev, E. F.; Schaefer, H. F.; Quack, M. *J. Chem. Phys.* **2002**, *116*, 690.
(40) Jurečka, P.; Šponer, J.; Černý, J.; Hobza, P. *Phys. Chem. Chem. Phys.* **2006**, *8*, 1985−93.
(41) Podeszwa, R.; Patkowski, K.; Szalewicz, K. *Phys. Chem. Chem. Phys.* **2010**, *12*, 5974−5979.
(42) Takatani, T.; Hohenstein, E. G.; Malagoli, M.; Marshall, M. S.; Sherrill, C. D. *J. Chem. Phys.* **2010**, *132*, 144104.
(43) Řezáč, J.; Riley, K. E.; Hobza, P. *J. Chem. Phys.* **2011**, *7*, 2427−2438.
(44) Thanthiriwatte, K. S.; Hohenstein, E. G.; Burns, L. A.; Sherrill, C. D. *J. Chem. Theory Comput.* **2011**, *7*, 88−96.
(45) Hobza, P. *Acc. Chem. Res.* **2012**, *45*, 663−672.
(46) Marshall, M. S.; Burns, L. A.; Sherrill, C. D. *J. Chem. Phys.* **2011**, *135*, 194102.
(47) Thiévin, J.; Cadudal, Y.; Georges, R.; Vigasin, A. *J. Mol. Spectrosc.* **2006**, *240*, 141−152.
(48) Pérez, C.; Muckle, M. T.; Zaleski, D. P.; Seifert, N. A.; Temelso, B.; Shields, G. C.; Kisiel, Z.; Pate, B. H. *Science* **2012**, *336*, 897−901.
(49) Suhm, M. A.; Kollipost, F. *Phys. Chem. Chem. Phys.* **2013**, *15*, 10702−10721.
(50) Pérez, C.; Lobsiger, S.; Seifert, N. A.; Zaleski, D. P.; Temelso, B.; Shields, G. C.; Kisiel, Z.; Pate, B. H. *Chem. Phys. Lett.* **2013**, *571*, 1−15.
(51) Zischang, J.; Suhm, M. A. *J. Chem. Phys.* **2013**, *139*, 024201.
(52) Otto, K. E.; Xue, Z.; Zielke, P.; Suhm, M. A. *Phys. Chem. Chem. Phys.* **2014**, *16*, 9849−9858.
(53) Buck, U.; Pradzynski, C. C.; Zeuch, T.; Dieterich, J. M.; Hartke, B. *Phys. Chem. Chem. Phys.* **2014**, *16*, 6859−6871.
(54) Miliordos, E.; Aprà, E.; Xantheas, S. S. *J. Chem. Phys.* **2013**, *139*, 114302.
(55) Mills, I. In *Molecular Spectroscopy: Modern Research*; Rao, N., Mathews, C., Eds.; Academic Press: New York, 1972; Vol. *1*, pp 115−140.
(56) Barone, V. *J. Chem. Phys.* **2005**, *122*, 014108.
(57) Vázquez, J.; Stanton, J. F. *Mol. Phys.* **2006**, *104*, 377−388.
(58) Barone, V.; Bloino, J.; Guido, C. A.; Lipparini, F. *Chem. Phys. Lett.* **2005**, *496*, 157−161.
(59) Schofield, D. P.; Kjaergaard, H. G. *Phys. Chem. Chem. Phys.* **2003**, *5*, 3100−3105.
(60) Schofield, D. P.; Lane, J. R.; Kjaergaard, H. G. *J. Phys. Chem. A* **2007**, *111*, 567−572.
(61) Salmi, T.; Hänninen, V.; Garden, A. L.; Kjaergaard, H. G.; Tennyson, J.; Halonen, L. *J. Phys. Chem. A* **2008**, *112*, 6305−6312.
(62) Kjaergaard, H. G.; Garden, A. L.; Chaban, G. M.; Gerber, R. B.; Matthews, D. A.; Stanton, J. F. *J. Phys. Chem. A* **2008**, *112*, 4324−4335.
(63) Garden, A. L.; Halonen, L.; Kjaergaard, H. G. *J. Phys. Chem. A* **2008**, *112*, 7439−47.
(64) Lane, J. R.; Kjaergaard, H. G. *J. Chem. Phys.* **2010**, *132*, 174304.
(65) Mackeprang, K.; Kjaergaard, H. G.; Salmi, T.; Hänninen, V.; Halonen, L. *J. Chem. Phys.* **2014**, *140*, 184309.
(66) Kalescky, R.; Zou, W.; Kraka, E.; Cremer, D. *Chem. Phys. Lett.* **2012**, *554*, 243−247.
(67) Lischka, H. *J. Am. Chem. Soc.* **1974**, *96*, 4761−4766.
(68) Yarkony, D. R. *J. Chem. Phys.* **1974**, *60*, 855.
(69) Lischka, H. *Chem. Phys. Lett.* **1979**, *66*, 108−110.
(70) Karpfen, A.; Beyer, A.; Schuster, P. *Int. J. Quantum Chem.* **1981**, *19*, 1113−1119.
(71) Gaw, J. F.; Yamaguchi, Y.; Vincent, M. A.; Schaefer, H. F., III *J. Am. Chem. Soc.* **1984**, *106*, 3133−3138.
(72) Frisch, M. J.; Del Bene, J. E.; Binkley, J. S.; Schaefer, H. F. *J. Chem. Phys.* **1986**, *84*, 2289.
(73) Latajka, Z.; Scheiner, S. *Chem. Phys.* **1988**, *122*, 413−430.
(74) Bishop, D. M.; Pipin, J.; Kirtman, B. *J. Chem. Phys.* **1995**, *102*, 6778.
(75) Collins, C. L.; Morihashi, K.; Yamaguchi, Y.; Schaefer, H. F. *J. Chem. Phys.* **1995**, *103*, 6051−6056.
(76) Peterson, K. A.; Dunning, T. H. *J. Chem. Phys.* **1995**, *102*, 2032.
(77) Tschumper, G. S.; Yamaguchi, Y.; Schaefer, H. F. *J. Chem. Phys.* **1997**, *106*, 9627−9633.
(78) Hobza, P.; Havlas, Z. *Collect. Czechoslov. Chem. Commun.* **1998**, *63*, 1343−1354.
(79) Halkier, A.; Klopper, W.; Helgaker, T.; Jørgensen, P.; Taylor, P. R. *J. Chem. Phys.* **1999**, *111*, 9157−9167.
(80) Tschumper, G. S.; Kelty, M. D.; Schaefer, H. F. *Mol. Phys.* **1999**, *96*, 493.
(81) Friedrich, J.; Perlt, E.; Roatsch, M.; Spickerman, C.; Kirchner, B. *J. Chem. Theory Comput.* **2011**, *7*, 843−851.
(82) Řezáč, J.; Hobza, P. *J. Chem. Theory Comput.* **2014**, *10*, 3066−3073.
(83) Kofranek, M.; Lischka, H.; Karpfen, A. *Chem. Phys.* **1988**, *121*, 136−153.
(84) Bunker, P.; Kofranek, M.; Lischka, H.; Karpfen, A. *J. Chem. Phys.* **1988**, *89*, 3002−3007.
(85) Bunker, P.; Jensen, P.; Karpfen, A.; Kofranek, M.; Lischka, H. *J. Chem. Phys.* **1990**, *92*, 7432−7440.
(86) Quack, M.; Suhm, M. A. *Chem. Phys. Lett.* **1990**, *171*, 517−524.
(87) Quack, M.; Suhm, M. A. *J. Chem. Phys.* **1991**, *95*, 28.
(88) Stanton, J. F.; Gauss, J.; Harding, M. E.; Szalay, P. G. *CFOUR, Coupled-Cluster techniques for Computational Chemistry*, with contributions from Auer, A. A.; Bartlett, R. J.; Benedikt, U.; Berger, C.; Bernholdt, D. E.; Bomble, Y.J.; Cheng, L.; Christiansen, O.; Heckert, M.; Heun, O.; Huber, C.; Jagau, T.-C.; Jonsson, D.; Jusélius, J.;Klein, K.; Lauderdale, W. J.; Matthews, D.A.; Metzroth, T.; Mück, L. A.; O'Neill, D. P.; Price, D. R.; Prochnow, E.; Ruud, K.; Schiffmann, F.; Schwalbach, W.; Stopkowicz, S.; Tajti, A.; Vázquez, J.; Wang, F.; Watts, J. D. and the integral packages MOLECULE (Almlöf, J. and Taylor, P. R.) and PROPS (Taylor, P. R.) and ABACUS (Helgaker, T.; Jensen, H. J. Aa.; Jørgensen, P.; Olsen, J.) and ECP routines by Mitin, A. V. and van Wüllen, C.. For the current version see http://www.cfour.de.
(89) Frisch, M. J.; Trucks, G. W.; Schlegel, H. B.; Scuseria, G. E.; Robb, M. A.; Cheeseman, J. R.; Scalmani, G.; Barone, V.; Mennucci, B.; Petersson, G. A.; Nakatsuji, H.; Caricato, M.; Li, X.; Hratchian, H. P.; Izmaylov, A. F.; Bloino, J.; Zheng, G.; Sonnenberg, J. L.; Hada, M.; Ehara, M.; Toyota, K.; Fukuda, R.; Hasegawa, J.; Ishida, M.; Nakajima, T.; Honda, Y.; Kitao, O.; Nakai, H.; Vreven, T.; Montgomery, A. J., Jr.; Peralta, J. E.; Ogliaro, F.; Bearpark, M.; Heyd, J. J.; Brothers, E.; Kudin, K. N.; Staroverov, V. N.; Kobayashi, R.; Normand, J.; Raghavachari, K.; Rendell, A.; Burant, J. C.; Iyengar, S. S.; Tomasi, J.; Cossi, M.; Rega, N.; Millam, J. M.; Klene, M.; Knox, J. E.; Cross, J. B.; Bakken, V.; Adamo, C.; Jaramillo, J.; Gomperts, R.; Stratmann, R. E.; Yazyev, O.; Austin, A. J.; Cammi, R.; Pomelli, C.; Ochterski, J. W.; Martin, R. L.; Morokuma, K.; Zakrzewski, V. G.; Voth, G. A.; Salvador, P.; Dannenberg, J. J.; Dapprich, S.; Daniels, A. D.; Farkas, O.; Foresman, J. B.; Ortiz, J. V.; Cioslowski, J.; Fox, D. J. *Gaussian09*, Revision D.01; Gaussian Inc.: Wallingford, CT, 2009.
(90) Schneider, W.; Thiel, W. *Chem. Phys. Lett.* **1989**, *157*, 367−373.
(91) Dunning, T. H., Jr. *J. Chem. Phys.* **1989**, *90*, 1007−1023.
(92) Werner, H.-J.; Knowles, P. J.; Manby, F. R.; Schütz, M.; Celani, P.; Knizia, G.; Korona, T.; Lindh, R.; Mitrushenkov, A.; Rauhut, G.; Adler, T. B.; Amos, R. D.; Bernhardsson, A.; Berning, A.; Cooper, D. L.; Deegan, M. J. O.; Dobbyn, A. J.; Eckert, F.; Goll, E.; Hampel, C.; Hesselmann, A.; Hetzer, G.; Hrenar, T.; Jansen, G.; Köppl, C.; Liu, Y.; Lloyd, A. W.; Mata, R. A.; May, A. J.; McNicholas, S. J.; Meyer, W.; Mura, M. E.; Nicklass, A.; Palmieri, P.; Pflüger, K.; Pitzer, R.; Reiher, M.; Shiozaki, T.; Stoll, H.; Stone, A. J.; Tarroni, R.; Thorsteinsson, T.;

Wang, M.; Wolf, A. *MOLPRO, version 2010.1, a package of ab initio programs*, 2010; see http://www.molpro.net.
(93) Turney, J. M.; Simmonett, A. C.; Parrish, R. M.; Hohenstein, E. G.; Evangelista, F. A.; Fermann, J. T.; Mintz, B. J.; Burns, L. A.; Wilke, J. J.; Abrams, M. L.; Russ, N. J.; Leininger, M. L.; Janssen, C. L.; Seidl, E. T.; Allen, W. D.; Schaefer, H. F.; King, R. A.; Valeev, E. F.; Sherrill, C. D.; Crawford, T. D. *Wiley Interdiscip. Rev.: Comput. Mol. Sci.* **2012**, *2*, 556−565.
(94) CFOUR Mailing List. https://lists.uni-mainz.de/sympa/arc/cfour/2012-08/msg00056.html (accessed Nov. 3, 2014).
(95) Lane, J. R.; Kjaergaard, H. G. *J. Chem. Phys.* **2009**, *131*, 034307.
(96) Tschumper, G. S. Reliable Electronic Structure Computations for Weak Non-Covalent Interactions in Clusters. In *Reviews in Computational Chemistry*; Lipkowitz, K. B., Cundari, T. R., Eds.; Wiley-VCH, Inc.: Hoboken, NJ, 2009; Vol. *26*, pp 39−90.
(97) von Puttkamer, K.; Quack, M. *Chem. Phys.* **1989**, *139*, 31−53.
(98) Matthews, D. A.; Vázquez, J.; Stanton, J. F. *Mol. Phys.* **2007**, *105*, 2659−2666.
(99) Quack, M.; Suhm, M. A. *Theor. Chim. Acta* **1996**, *93*, 61−65.
(100) Anderson, D. T.; Davis, S.; Nesbitt, D. J. *J. Chem. Phys.* **1996**, *104*, 6225−6243.
(101) Pine, A. S.; Lafferty, W. J.; Howard, B. J. *J. Chem. Phys.* **1984**, *81*, 2939.
(102) Miller, R. *Acc. Chem. Res.* **1990**, *23*, 10−16.
(103) Anderson, D. T.; Davis, S.; Nesbitt, D. J. *J. Chem. Phys.* **1996**, *105*, 4488.
(104) Hippler, M.; Oeltjen, L.; Quack, M. *J. Phys. Chem. A* **2007**, *111*, 12659−12668.
(105) Suhm, M. A.; Farrell, J. T., Jr.; McIlroy, A.; Nesbitt, D. J. *J. Chem. Phys.* **1992**, *97*, 5341−5354.
(106) Huisken, F.; Kaloudis, M.; Kulcke, A. *J. Chem. Phys.* **1996**, *104*, 17−25.
(107) Braly, L.; Liu, K.; Brown, M.; Keutsch, F.; Fellers, R.; Saykally, R. *J. Chem. Phys.* **2000**, *112*, 10314−10326.
(108) Keutsch, F. N.; Braly, L. B.; Brown, M. G.; Harker, H. A.; Petersen, P. B.; Leforestier, C.; Saykally, R. J. *J. Chem. Phys.* **2003**, *119*, 8927−8937.
(109) Bouteiller, Y.; Perchard, J. *Chem. Phys.* **2004**, *305*, 1−12.
(110) Rocher-Casterline, B. E.; Ch'ng, L. C.; Mollner, A. K.; Reisler, H. *J. Chem. Phys.* **2011**, *134*, 211101.
(111) Huisken, F.; Kaloudis, M.; Vigasin, A. *Chem. Phys. Lett.* **1997**, *269*, 235−243.
(112) Groenenboom, G.; Wormer, P.; van der Avoird, A.; Mas, E.; Bukowski, R.; Szalewicz, K. *J. Chem. Phys.* **2000**, *113*, 6702−6714.
(113) Nizkorodov, S. A.; Ziemkiewicz, M.; Nesbitt, D. J. *J. Chem. Phys.* **2005**, *122*, 194316.
(114) Ptashnik, I. V.; Smith, K. M.; Shine, K. P.; Newnham, D. A. *Q. J. R. Meteorol. Soc.* **2004**, *130*, 2391−2408.